



# RPA-mediated recruitment of Bre1 couples histone H2B ubiquitination to DNA replication and repair

Guangxue Liu<sup>a</sup>, Jiaqi Yan<sup>a</sup>, Xuejie Wang<sup>a</sup>, Junliang Chen<sup>b</sup>, Xin Wang<sup>a</sup> , Yang Dong<sup>a</sup>, Simin Zhang<sup>a</sup>, Xiaoli Gan<sup>a</sup>, Jun Huang<sup>b</sup>, and Xuefeng Chen<sup>a,1</sup>

<sup>a</sup>Hubei Key Laboratory of Cell Homeostasis, Department of Genetics, College of Life Sciences and Institute for Advanced Studies, Wuhan University, 430072 Wuhan, China; and <sup>b</sup>The MOE Key Laboratory of Biosystems Homeostasis & Protection, Zhejiang Provincial Key Laboratory for Cancer Molecular Cell Biology and Innovation Center for Cell Signaling Network, Life Sciences Institute, Zhejiang University, 310058 Hangzhou, China

Edited by James E. Haber, Brandeis University, Waltham, MA, and approved January 21, 2021 (received for review August 18, 2020)

**The ubiquitin E3 ligase Bre1-mediated H2B monoubiquitination (H2Bub) is essential for proper DNA replication and repair in eukaryotes. Deficiency in H2Bub causes genome instability and cancer. How the Bre1–H2Bub pathway is evoked in response to DNA replication or repair remains unknown. Here, we identify that the single-stranded DNA (ssDNA) binding factor RPA acts as a key mediator that couples Bre1-mediated H2Bub to DNA replication and repair in yeast. We found that RPA interacts with Bre1 in vitro and in vivo, and this interaction is stimulated by ssDNA. This association ensures the recruitment of Bre1 to replication forks or DNA breaks but does not affect its E3 ligase activity. Disruption of the interaction abolishes the local enrichment of H2Bub, resulting in impaired DNA replication, response to replication stress, and repair by homologous recombination, accompanied by increased genome instability and DNA damage sensitivity. Notably, we found that RNF20, the human homolog of Bre1, interacts with RPA70 in a conserved mode. Thus, RPA functions as a master regulator for the spatial–temporal control of H2Bub chromatin landscape during DNA replication and recombination, extending the versatile roles of RPA in guarding genome stability.**

Bre1 | H2B ubiquitination | RPA | DNA replication | homologous recombination

**P**roper DNA replication and maintenance of genome stability are essential for cell proliferation and faithful transmission of genetic information to daughter cells. Collapsed replication forks or replication through single-stranded DNA (ssDNA) gap can generate DNA double-stranded breaks (DSBs), one of the most cytotoxic DNA lesions threatening genome stability. Defects in DNA replication or DSB repair can cause genome instability and human diseases, including cancer (1, 2).

Homologous recombination (HR) is a universally conserved mechanism for repairing DSBs or restarting stalled or collapsed replication forks (3–5). Defects in HR can lead to somatic cell transformation and oncogenesis in mammals (6, 7). HR repairs DSBs by copying a DNA sequence from a homologous template, usually a sister chromatid. During HR, the 5'-terminated strand of DSBs is processed to generate 3'-tailed ssDNA (3, 5, 8). The 3'-end ssDNA is bound by the heterotrimeric ssDNA binding factor replication protein A (RPA) to activate the DNA damage checkpoint (9). Subsequently, Rad51 recombinase replaces the RPA bound on ssDNA to form a Rad51 nucleoprotein filament (4, 10). The Rad51–ssDNA filament catalyzes invasion of a homologous sequence to form the D-loop structure, followed by repair DNA synthesis and resolution of recombination intermediates (3, 4, 10).

Eukaryotic cells have evolved a complex signaling network that integrates a plethora of protein posttranslational modifications to ensure proper DNA replication and repair. A central player among these events is the monoubiquitination of histone H2B (H2Bub) that is essential for proper DNA replication, repair, and transcription across species (11–22). H2Bub acts to decompact chromatin or regulate nucleosome dynamics to allow DNA access by protein machinery (14, 17, 18, 23, 24). H2Bub is also required for

meiosis, mitotic chromosome segregation, and maintenance of centromere and telomere (25–30). Thus, H2Bub locates in the center of the regulatory network that controls all essential processes in the nucleus. In yeast, this modification is catalyzed by the E2 ubiquitin conjugase Rad6 (Ubc6 or RAD6 in human) in cooperation with the E3 ubiquitin ligase Bre1 (RNF20/RNF40 in mammals) (20–22, 31, 32). The modification occurs on K123 in budding yeast, K119 in *Schizosaccharomyces pombe*, and K120 in mammals (24).

During DNA replication, Bre1 is recruited to replication forks to stimulate local H2Bub, which is required to promote replication fork progression, DNA synthesis, and nucleosome assembly on newly replicated DNA (14). Upon replication stresses, H2Bub facilitates the stabilization of replication forks, bypassing DNA lesions, and recovery from the stress (12–14). In mouse cells, depletion of RNF20/RNF40, the homolog of yeast Bre1, causes replication stresses due to the accumulation of R-loop, a DNA–RNA hybrid that impedes DNA replication and leads to genome instability (16). Upon the induction of DSBs, Bre1 is recruited to DSB ends to stimulate local H2Bub that allows efficient Rad51 loading and HR repair, likely by facilitating local histone eviction (24). Similarly, RNF20/RNF40 is recruited to DSB ends in human cells. RNF20-dependent H2Bub is critical to promote HR repair and class switch recombination via stimulating chromatin relaxation and recruitment of downstream repair proteins (15, 17, 18, 33). As a result, cells lacking Bre1 or RNF20 are sensitive to ionizing radiation or DNA-damaging agents (33–36). These studies place Bre1- or

## Significance

**In eukaryotes, the monoubiquitination of histone H2B (H2Bub) plays a critical role in shaping chromatin structure, dynamics, and function. This modification is essential for proper DNA replication, repair, and transcription, but how H2Bub is evoked during these processes is unknown. Here, we found that the single-stranded DNA sensor RPA recruits Bre1, the ubiquitin E3 ligase for H2Bub, to replication forks or DNA breaks to stimulate local H2Bub. We show that RPA-mediated Bre1 recruitment is essential to promote DNA replication and repair by homologous recombination while suppressing mutations and genome instability. Thus, we reveal that RPA couples H2Bub to DNA replication and repair and controls the spatial–temporal distribution of H2Bub on chromatin.**

Author contributions: G.L. and X.C. designed research; G.L., J.Y., Xuejie Wang, Xin Wang, Y.D., S.Z., and X.G. performed research; J.C. and J.H. designed and performed immunoprecipitations for testing RNF20–RPA70 interaction in vivo; G.L. and X.C. analyzed data; and X.C. wrote the paper.

The authors declare no competing interest.

This article is a PNAS Direct Submission.

Published under the PNAS license.

<sup>1</sup>To whom correspondence may be addressed. Email: xfchen@whu.edu.cn.

This article contains supporting information online at <https://www.pnas.org/lookup/suppl/doi:10.1073/pnas.2017497118/-DCSupplemental>.

Published February 18, 2021.

RNF20/RNF40-mediated H2Bub at the forefront of the DNA damage response, serving as a key barrier against genome instability and cancer formation. However, a key question that remains unanswered is how the Bre1–H2Bub pathway is evoked to respond to the DNA replication and repair processes.

In this study, we searched for the Bre1-interacting proteins and found that the ssDNA binding factor RPA physically interacts with Bre1 in yeast. RPA functions as a critical sensor of ssDNA to coordinate DNA replication, repair, and recombination, and it is essential for all DNA transactions (37, 38). We found that RPA directly interacts with Bre1 and recruits the enzyme to replication origins in the S phase or to DSB ends upon DNA damage. The RPA-mediated recruitment of Bre1 is essential to stimulate local H2B ubiquitination and ensure proper DNA replication, nucleosome assembly, and HR repair, thus preserving genome stability. Notably, we found that human RNF20 also interacts with RPA, and we identified a pair of conserved motifs that mediate the RPA–Bre1/RNF20 interaction. Thus, we reveal RPA as the key mediator coupling the Bre1–H2Bub pathway to DNA replication and HR repair. Our results suggest that this mechanism is likely conserved in humans.

## Results

**Bre1 Interacts with RPA In Vivo and In Vitro.** Given the importance of Bre1-dependent H2Bub in DNA replication and repair (12–14, 17, 18, 24), we aimed to address how Bre1 is spatiotemporally controlled to ensure its timely recruitment to replication forks or

DNA damage sites. We treated yeast cells with methylmethane sulfonate (MMS) to induce replication stresses or DNA damage and performed Bre1-3xFLAG immunoprecipitation. An untagged strain treated with MMS was used as a control. We identified Bre1-associated proteins by mass spectrometry analysis. Among the top hits, we identified Rad6, Ssb2, Rfa1, Pgk1, and Dpb2 (Fig. 1A). Rfa1, the large subunit of the RPA complex, was highly enriched in the immunoprecipitation products relative to the control. Given the versatile roles of RPA in the DNA damage response, we went on to verify the interaction. Indeed, we found that Rfa1-3xHA interacts with Bre1-3xFLAG in vivo, specifically in a salt-sensitive manner (Fig. 1B). Interestingly, we observed that this interaction appears to occur primarily in the S and G2/M phases (Fig. 1C and *SI Appendix, Fig. S1*). Notably, the interaction was enhanced upon hydroxyurea (HU) or MMS treatment (Fig. 1D). Next, we expressed the recombinant GST-Bre1 and 6xHis-Rfa1 proteins and tested their association by pull-down assay. As expected, 6xHis-Rfa1 interacts directly with GST-Bre1 in a dose-dependent manner in vitro (Fig. 1E).

### ssDNA Stimulates the Physical Interaction between RPA and Bre1.

Since RPA specifically binds ssDNA on chromatin, we examined whether Bre1 binds the RPA–ssDNA nucleoprotein complex by streptavidin pull-down assay. Biotin-labeled ssDNA (90 nucleotides [nt]) was immobilized to streptavidin magnetic beads. In the absence of RPA, ssDNA alone fails to capture Bre1, indicating that Bre1 does not bind ssDNA (Fig. 1F, lane 5). However, once

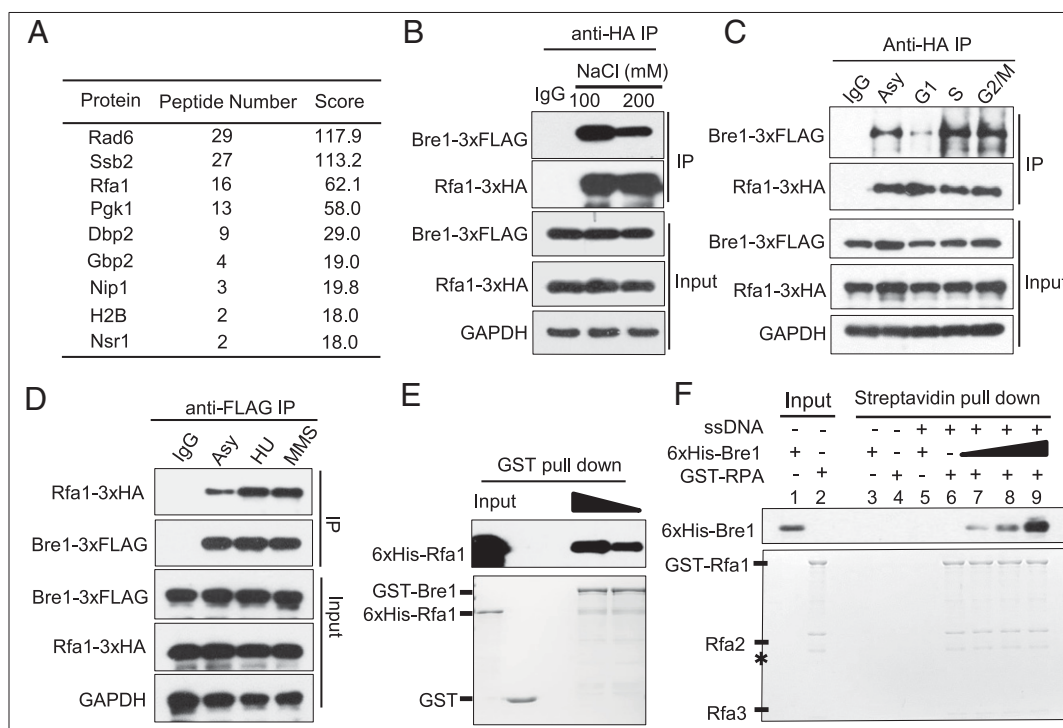


**Fig. 1.** Bre1 interacts with RPA in vivo and in vitro. (A) Table showing Bre1-associated proteins identified by mass spectrometry analysis. The unique peptide number for each identified protein is indicated. The score is an indicator of reliability. (B–D) Immunoprecipitation and Western blot analysis of the interaction between Rfa1-3xHA and Bre1-3xFLAG at indicated conditions. Glyceraldehyde-3-phosphate dehydrogenase (GAPDH) serves as a loading control. Alpha factor (5  $\mu$ g/mL), HU (200 mM), or nocodazole (10  $\mu$ g/mL) was used to arrest cells at the G1, S, and G2/M phase, respectively. To induce replication stress or DNA damage, cells were treated with HU (200 mM) for 2 h or MMS (0.1%) for 1 h before collection. Asynchronous cells (Asy) were used as control. (E) GST pull-down assay showing the interaction between GST-Bre1 and 6xHis-Rfa1. GST-Bre1 was immobilized on beads to capture the 6xHis-Rfa1 protein. GST was used as a negative control. (Bottom) Coomassie blue staining of GST-Bre1 or GST used for the experiment. (Top) A Western blot showing the amount of 6xHis-Rfa1 captured by GST-Bre1. The arrow indicates that a gradient amount of 6xHis-Rfa1 was used for the experiment. (F) A streptavidin pull-down assay shows the association between 6xHis-Bre1 and RPA–ssDNA complex; 50 pM of 5'-biotinylated ssDNA (90 nt) was immobilized on streptavidin beads before adding 50 nM of purified yeast GST–RPA complex. An increasing amount of 6xHis-Bre1 was added to the mixture containing ssDNA or RPA–ssDNA complex. (Bottom) Coomassie blue staining of the RPA used for the experiments (lanes 6–9). (Top) A Western blot showing the amount of 6xHis-Bre1 associated with GST–RPA–ssDNA. Asterisk denotes degraded RPA fragments.

RPA is preincubated with the ssDNA immobilized to beads we detected a dose-dependent binding of Bre1 to the RPA-ssDNA complex (lanes 7 to 9). To test whether ssDNA affects the binding of Bre1 to RPA, we incubated GST-RPA with various amounts of ssDNA and then added a constant amount of 6xHis-Bre1. GST pull-down assay showed that the addition of ssDNA enhances the association between Bre1 and RPA (*SI Appendix, Fig. S2*, lanes 4 to 6). Thus, Bre1 binds RPA or RPA-ssDNA both in vivo and in vitro, and this interaction is stimulated by ssDNA.

**Identification of the Residues that Mediate the RPA-Bre1 Interaction.** Bre1 is composed of a Rad6-binding domain (RBD), a RING domain, and a linker region that bridges the RBD and the RING domains (Fig. 2*A*). To map the specific domain that mediates the association with RPA, we expressed GST-tagged RBD, RING, and the linker and tested their abilities for binding 6xHis-Rfa1 by GST pull-down assay. We found that the linker region (211 to 614 amino acids [aa]) but not the RBD (1 to 210 aa) or the RING domain (615 to 700 aa) interacts with Rfa1 (Fig. 2*A* and *B*). Next, we generated a series of truncations for the linker region. We observed that the fragments starting from residue 211 to residue 431, 459, 465, 479, or 500 all failed to interact with Rfa1, while the one from 211 to 522 can weakly bind Rfa1 (Fig. 2*C*), suggesting

that the region between residues 500 and 522 is required for mediating the interaction. This region is located outside the predicted coiled-coil domains (*SI Appendix, Fig. S3*). Sequence alignment showed that Bre1 and its orthologs share a conserved motif within this region (*SI Appendix, Fig. S44*). Indeed, mutation of the two acidic residues D520 and D522 to alanine greatly impaired the interaction, while simultaneous mutation of the six residues (L516, L518, D520, D522, L524, and L525) in Bre1 to alanine (bre1-6A) completely abolished the interaction with RPA (Fig. 2*D*). As expected, bre1-6A failed to bind the RPA-ssDNA complex in vitro (*SI Appendix, Fig. S5*). Accordingly, the bre1-6A mutant protein does not interact with Rfa1 in vivo, either (Fig. 2*E*). Thus, we defined the Bre1 motif (LxLxD/ExD/ExLL) (x can be any amino acid) that mediates the RPA-Bre1 interaction.

Next, we turned to delineate the motif in Rfa1 that mediates its interaction with Bre1. We expressed 6xHis-tagged full-length Rfa1 or OB-A, OB-B, or OB-C motif and tested their binding to GST-Bre1 (Fig. 2*F*). We noted that only the full-length Rfa1 and the OB-C motif could interact with Bre1 (Fig. 2*G*). Next, we expressed a series of truncated OB-C domains and tested their affinities for Bre1. We observed that the fragment R450 (1 to 450 aa) or R1 (1 to 436 aa) does not bind Bre1, while the fragment R477 (1 to 477 aa) or R508 (1 to 508 aa) can interact with Bre1 (Fig. 2*H*),

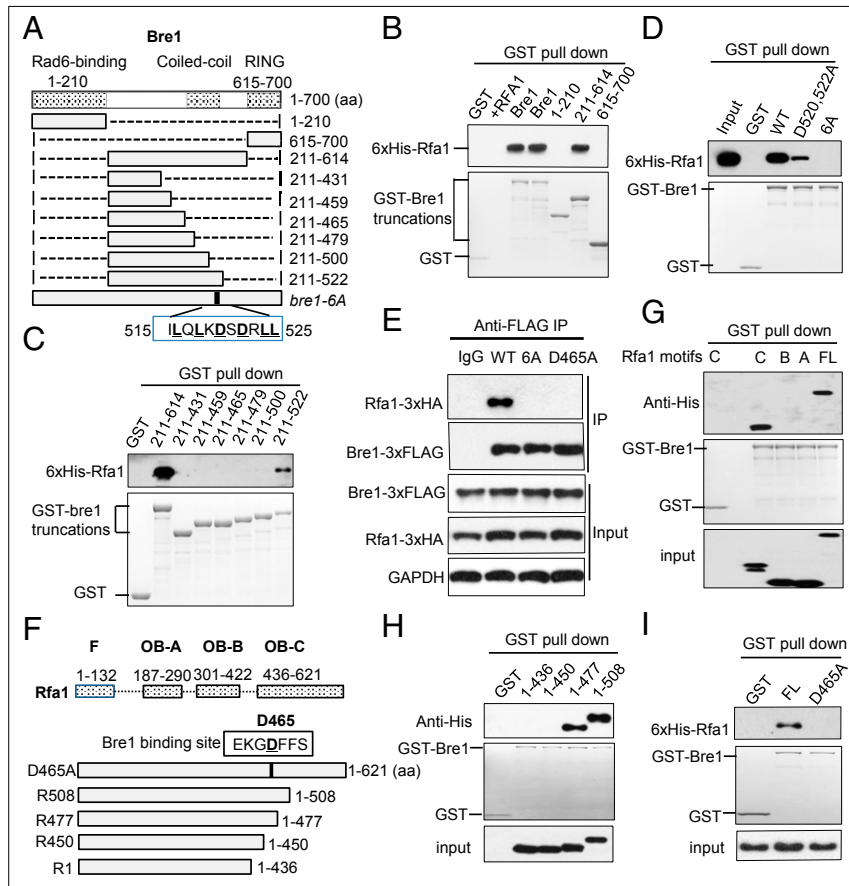


**Fig. 2.** Identification of the residues that mediate the RPA-Bre1 interaction. (*A*) Scheme showing the full-length or truncated Bre1 proteins used for pull-down assays. Dashed lines represent deleted regions, while the gray bars represent the truncated Bre1 proteins. The exact positions for these truncations are indicated. The RPA-interacting motif of Bre1 is shown in the box, and the key residues are marked in bold. (*B–D*) GST pull-down assay showing the interaction between 6xHis-Rfa1 and the WT, truncated, or mutated GST-Bre1 proteins. GST was used as a negative control. The amount of WT or mutant GST-Bre1 protein used for experiments is indicated by Coomassie blue staining of an SDS-PAGE (*Bottom*). The associated 6xHis-Rfa1 was detected by Western blot with an anti-His antibody (*Top*). (*E*) Immunoprecipitation analysis indicating the interaction between Bre1-3xFLAG, bre1-6A-3xFLAG, and Rfa1-3xHA or rfa1-D465A-3xHA. (*F*) Graph showing the motifs of the full-length or truncated Rfa1 protein used for pull-down assays. (*G–I*) GST pull-down assays showing the association between GST-Bre1 and 6xHis tagged full-length, truncated or mutated Rfa1 proteins. The amount of GST-Bre1 used for experiments is indicated by Coomassie blue staining (*Middle*). The WT or mutant 6xHis-Rfa1 associated with GST-Bre1 was detected by Western blot with an anti-His antibody (*Top*).

suggesting that the region between 450 aa and 477 aa is critical for the association. Therefore, we mutated the conserved amino acids located in this region (*SI Appendix, Fig. S4B*). Eventually, we found that mutation of the single residue D465 to alanine (D465A) is sufficient to disrupt the Rfa1–Bre1 interaction in vitro and in vivo (Fig. 2 *E* and *I*). Thus, D465 of Rfa1 is critical to mediate the interaction with Bre1.

**Bre1–H2Bub Enrichment at Replication Forks Depends on the RPA–Bre1 Association.** RPA is known to be involved in replication initiation and elongation (38, 39). Indeed, upon release of the G1-arrested wild-type (WT) cells into media containing HU, we detected robust RPA recruitment at the early fired origins ARS305 or ARS607 but not at the late origin ARS610. Importantly, RPA loading did not decrease in the *bre1-6A* or *rfa1-D465A* mutant cells at early origins (Fig. 3*A*), indicating that the recruitment of RPA at replication forks is independent of its association with Bre1.

Corroborating with the role of H2Bub in replication, we detected the enrichment of Bre1 at the active origins ARS305 and ARS607 but not at the late origin ARS610 upon releasing the G1 cells into media with HU (Fig. 3*B*). However, the *bre1-6A* mutant protein was not recruited at these origins. Notably, Bre1 also failed to be recruited in the *rfa1-D465A* mutant (Fig. 3*B*). This is not due to any reduction of the Bre1 protein level in these mutants (*SI Appendix, Fig. S6*). Consistently, we detected a steady increase of H2Bub at active origins in the WT cells but not in *bre1-6A* or *rfa1-D465A* mutant cells upon entering into the S phase (Fig. 3*C*). Thus, the association with RPA is essential for Bre1 recruitment and subsequent H2Bub enrichment at replication origins or stalled forks. Interestingly, Bre1 appears to persist on chromatin at 120 min, when RPA localization has decreased (Fig. 3*A* and *B*), suggesting that additional mechanisms for recruiting or stabilizing Bre1 on daughter strands exist. It is worth noting that the failure to detect RPA, Bre1, or H2Bub at late origins is presumably due to activation of the replication checkpoint by HU, which is known to suppress the late origins (40).

Next, we tested whether the global H2Bub level is altered in these mutant cells. In unperturbed conditions, both WT and *bre1-6A* or

*rfa1-D465A* mutant cells have a comparable level of H2Bub (*SI Appendix, Fig. S7*). As a control, H2Bub was absent in the *bre1Δ* mutant cells. Importantly, blockage of cells in the S phase with HU resulted in a sharp increase of H2Bub in the WT cells. However, it only led to a very limited increase of H2Bub in the *bre1-6A* or *rfa1-D465A* mutant cells. Thus, the association between Bre1 and RPA is essential for the global increase of H2Bub at replication forks during DNA replication or upon replication stresses (*SI Appendix, Fig. S7*).

**The Association of Bre1 with RPA–ssDNA Does Not Alter Its E3 Ligase Activity.** To test whether *bre1-6A* mutation impairs its E3 ligase activity, we purified the ubiquitin E1 activating enzyme (Uba1), E2 conjugase (Rad6), and the E3 ligase (Bre1) and carried out an in vitro ubiquitination assay (*SI Appendix, Fig. S8A*). The nucleosome core particles (NCP) prepared from the *bre1Δ* mutant cells were used as a substrate. We noted that H2B was mono-ubiquitinated to a similar level in the presence of WT or mutant Bre1 protein, suggesting that the point mutation does not alter Bre1 ligase activity (*SI Appendix, Fig. S8B*). Furthermore, we examined the effect of RPA–ssDNA on Bre1-mediated H2B ubiquitination. We observed that the addition of RPA–ssDNA into the reaction did not change the level of H2Bub (*SI Appendix, Fig. S8C*). Thus, the association with RPA is not required for the E3 ligase activity of Bre1. Therefore, the reduction of H2Bub at replication forks in the *bre1-6A* or *rfa1-D465A* mutant was caused by decreased Bre1 recruitment.

**The RPA–Bre1 Interaction Facilitates DNA Replication and Represses Spontaneous DNA Damages.** We assessed the role of the RPA–Bre1 interaction on DNA replication. The G1-arrested WT, *bre1-6A*, *rfa1-D465A*, or *bre1Δ* cells were released to media without HU. Compared to the WT cells, the progression of the S phase was delayed for ~20 min in *bre1-6A* or *rfa1-D465A* mutant, and the defect was more pronounced in the *bre1Δ* mutant cells (Fig. 4*A*). Next, we monitored the incorporation of BrdU (5-bromo-2'-deoxyuridine), the analog of thymidine, into newly synthesized DNA. By chromatin immunoprecipitation (ChIP) qPCR, we detected robust

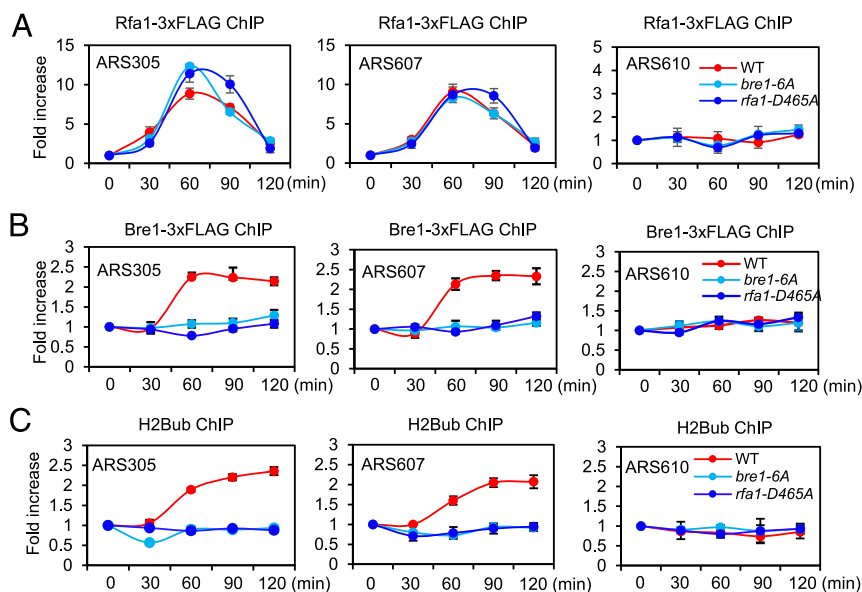


**Fig. 3.** RPA recruits Bre1 to replication origins to stimulate local H2B ubiquitination. (A) ChIP qPCR analysis of RPA-3xFLAG loading at indicated replication origins in the WT, *bre1-6A*, or *rfa1-D465A* cells. ARS305 and ARS607 are representative early-fired origins, while ARS610 is a typical late-fired origin. G1-arrested cells were released into media with 200 mM HU to block cells in the S phase. Samples were collected every 30 min. (B and C) ChIP qPCR showing the kinetics of Bre1-3xFLAG or H2Bub enrichment at indicated origins in the WT, *bre1-6A*, or *rfa1-D465A* cells. All ChIP signals were first normalized to the corresponding input signal, and then the derived ChIP/input values were normalized to that of the “0” time-point sample. Error bars represent the SD from three independent experiments.

BrdU enrichment at the active origins ARS305 and ARS607 but not at the late origin ARS610 in the WT cells. However, BrdU incorporation was significantly impaired in *bre1-6A* or *rfa1-D465A* mutant cells (Fig. 4B). Thus, the association of Bre1 with RPA is important for S-phase progression and DNA synthesis.

In parallel, histone H2B was properly assembled after DNA synthesis at the origins ARS305 and ARS607 in the WT cells. However, H2B assembly was delayed in the *bre1-6A* or *rfa1-D465A* mutant cells (Fig. 4C). These results indicate that the mutant cells have defects in DNA replication that further leads to a delay in nucleosome assembly. Consequently, the *bre1-6A* or *rfa1-D465A* mutant had a much higher level (25%~28%) of spontaneous DNA lesions than the WT cells (4%), as reflected by the Rad52-YFP (yellow fluorescent protein) foci, an indicator of DNA lesions (Fig. 4D). These spontaneous DNA lesions primarily result from improper DNA replication since they peaked in the S phase. Thus, the RPA–Bre1 association is crucial for targeting Bre1 to replication

forks to ensure proper DNA replication and nucleosome assembly while suppressing the spontaneous DNA damage.

**Disruption of the RPA–Bre1 Interaction Impairs Cellular Responses to Replication Stress.** Next, we evaluated the role of the RPA–Bre1 association in the cellular response to replication stress. G1-synchronized cells were released into the S phase in the presence of 200 mM HU. Compared to the WT cells, the *bre1-6A* or *rfa1-D465A* mutant exhibited severe delay (~40 min) in the cell-cycle progression (Fig. 4A). Further, we monitored the kinetics of Rad52 foci formation during the recovery from HU treatment. HU treatment resulted in a greater increase of DNA lesions in *bre1-6A* (24%) or *rfa1-D465A* (20%) cells than in the WT cells (12%). Upon HU removal, both mutants recovered with much slower kinetics than the WT cells (Fig. 5A and B). This result was confirmed by analysis of chromosome integrity using pulsed-field gel electrophoresis (PFGE) (Fig. 5C). These results suggest that

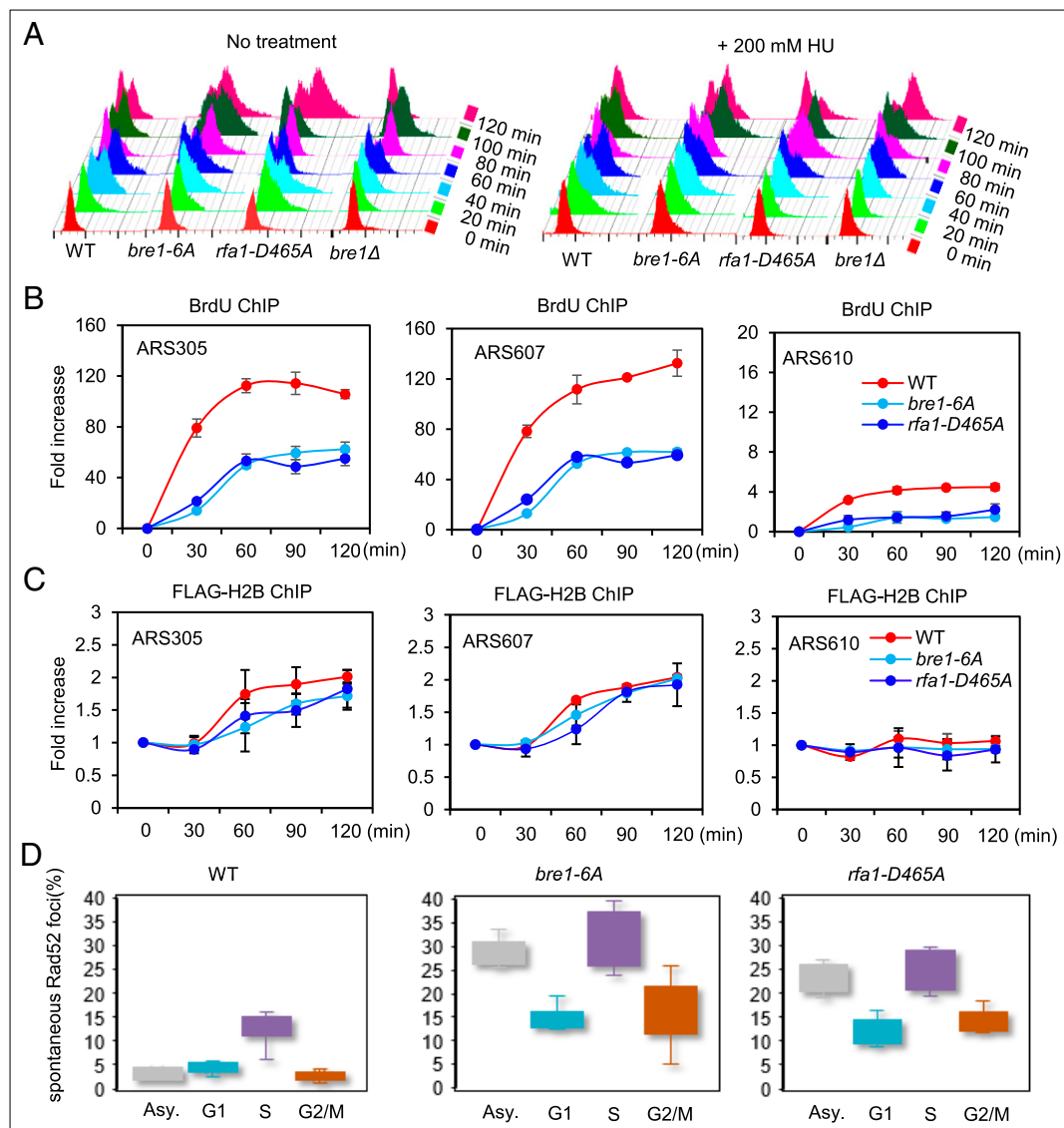


**Fig. 4.** RPA–Bre1 interaction facilitates DNA replication and represses spontaneous DNA damage. (A) Progression of the cell cycle monitored by flow cytometry for indicated cells. G1-arrested cells were released into fresh YPD media with or without HU (200 mM). Samples were collected every 20 min. (B) ChIP qPCR analysis of DNA synthesis, as reflected by BrdU incorporation. (C) ChIP analysis of histone H2B occupancy in indicated cells. ChIP signals in B and C were normalized to the corresponding input signals, and the derived ChIP/input values were normalized to that of the “0” time-point sample. (D) Plot showing the ratio of spontaneous Rad52-YFP foci at indicated cell cycle stages in indicated cells. Error bars represent the SD from at least three independent experiments.

these mutants have defects in repairing DNA lesions that arose from stalled or collapsed forks. Consistently, the *bre1-6A* or *rfa1-D465A* mutant exhibited hypersensitivity to MMS, HU, and camptothecin that can impede replication and cause replication stresses (Fig. 5D). Thus, RPA–Bre1 interaction is vital for cells to respond to and recover from replication stresses.

Notably, we found that similar to the *bre1-6A* mutant blockage of H2B ubiquitination by the *H2B-K123R* mutation also caused a defect in the S-phase progression in unperturbed conditions or under replication stress, and the defect is comparable to that seen in the *bre1-6A H2B-K123R* double mutant (SI Appendix, Fig. S9A and B). Consistently, the *bre1-6A* or *H2B-K123R* single mutant displayed a similar sensitivity to HU, as observed in the *bre1-6A H2B-K123R* double mutant (SI Appendix, Fig. S9C). Thus, the above defects seen in *bre1-6A* or *rfa1-D465A* cells are related to impaired H2Bub.

**RPA Mediates the Recruitment of Bre1 at DSB Ends.** Our previous studies revealed that Bre1 is recruited to DSB ends to stimulate local H2B ubiquitination and repair by HR (24). To examine whether Bre1 recruitment at DSBs also relies on RPA, we employed an unreparable system wherein a single HO-induced DSB is generated at the *MAT* locus on chromosome III upon galactose induction (41, 42). The donor sequences *HML* and *HMR* were deleted so that the cells cannot be repaired by HR. As expected, RPA was robustly recruited at DSB ends in the WT, *bre1-6A*, or *rfa1-D465A* cells (Fig. 6A). However, its recruitment was impaired in the *bre1Δ* mutant (Fig. 6A) (24). In line with previous reports, Bre1-3xFLAG was efficiently recruited to DSBs in the WT cells (24), but its recruitment was significantly reduced in both *bre1-6A* and *rfa1-D465A* cells (Fig. 6B). Notably, the DSB-induced enrichment of H2Bub was abolished in both *bre1-6A* and *rfa1-D465A* mutants (Fig. 6C), as seen in *bre1Δ* cells. Thus, the RPA–Bre1 interaction is critical for the enrichment of Bre1 and H2Bub at DSBs. The residual Bre1 loading at DSBs in *bre1-6A*

and *rfa1-D465A* cells may depend on other recruitment mechanisms or reflect H2Bub-independent functions. Indeed, the RING domain of Bre1 was reported to directly bind the acidic patch of nucleosomes (43, 44).

**The RPA–Bre1 Interaction Is Not Required for Checkpoint Activation upon DSBs.** In line with RPA loading status, the DSB-induced checkpoint activation, as mirrored by Rad53 phosphorylation, was normal in *bre1-6A* or *rfa1-D465A* cells but was deficient in *bre1Δ* cells (SI Appendix, Fig. S10A). Consistently, recruitment of the checkpoint adaptor protein Rad9 was proficient in the WT or *bre1-6A* cells but not in *bre1Δ* cells (SI Appendix, Fig. S10B). This difference may relate to the presence of a basal level of H2Bub in *bre1-6A* cells (SI Appendix, Fig. S7), given that H2Bub is known to promote H3K79 methylation that is required for Rad9 recruitment and checkpoint activation (32, 45). Therefore, unlike *BRE1* deletion mutant, disruption of the RPA–Bre1 interaction does not impair the DSB-induced checkpoint activation. Notably, the deficient checkpoint in *bre1Δ* cells appears to be an important reason leading to the defect of RPA loading in this mutant, since deletion of the genes encoding the checkpoint kinases Mec1 and Tel1 or the checkpoint adaptor Rad9 also impaired RPA loading (SI Appendix, Fig. S10C).

**RPA Targets Bre1 to DSBs to Promote DSB Repair by HR.** Next, we tested the role of RPA–Bre1 interaction on DSB repair by HR. Specifically, we employed an ectopic recombination system wherein a single HO cut is generated on chromosome V that can be repaired by using the homologous sequence on chromosome III as a donor (Fig. 6D) (46). Approximately 83% of WT cells repaired the break and survived, while only ~52% of *bre1-6A* or *rfa1-D465A* mutant cells survived (Fig. 6E), comparable to that observed in *bre1Δ* cells. Accordingly, the repair kinetics was slower in both point mutants than in the WT cells (Fig. 6F and G). In line with the HR defect, the loading of Rad51 was impaired in *bre1-6A* or *rfa1-D465A* cells (SI Appendix, Fig. S11). Thus, the

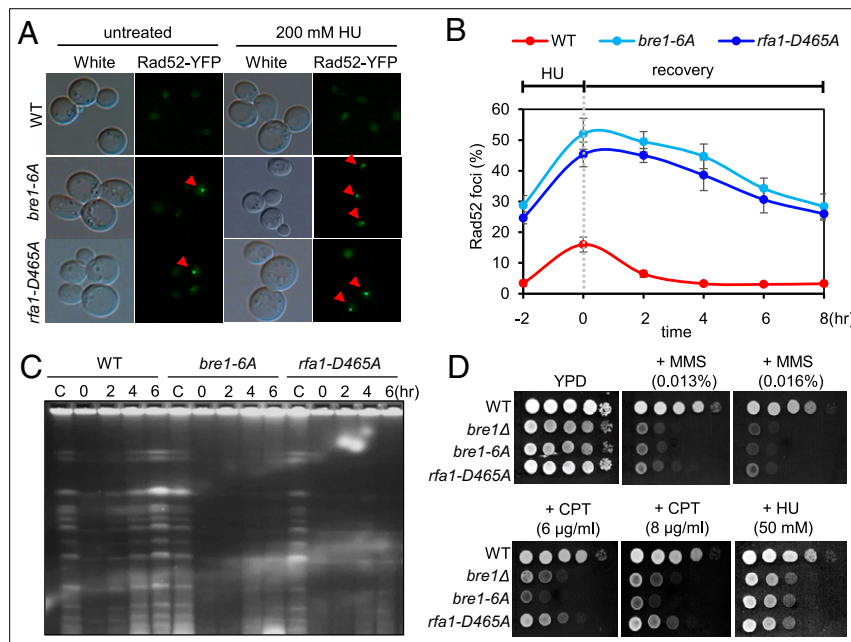


**Fig. 5.** The RPA–Bre1 association is critical for the response to replication stresses. (A and B) Microscopy analysis and quantification of cells harboring Rad52-YFP foci upon HU treatment or during the recovery. Cells were treated with 200 mM HU for 2 h followed by releasing into media without HU to allow the recovery. Rad52-YFP foci indicated by arrows were monitored at indicated time points. A representative image at 8 h is presented. Error bars represent the SD from three independent experiments. (C) Analysis of chromosome integrity using PFGE for indicated strains. Cells pretreated with 200 mM HU (for 2 h) were released into media without HU. Untreated cells (C) were used as control. (D) Spotting assay showing the sensitivity to MMS or camptothecin (CPT) for indicated cells.

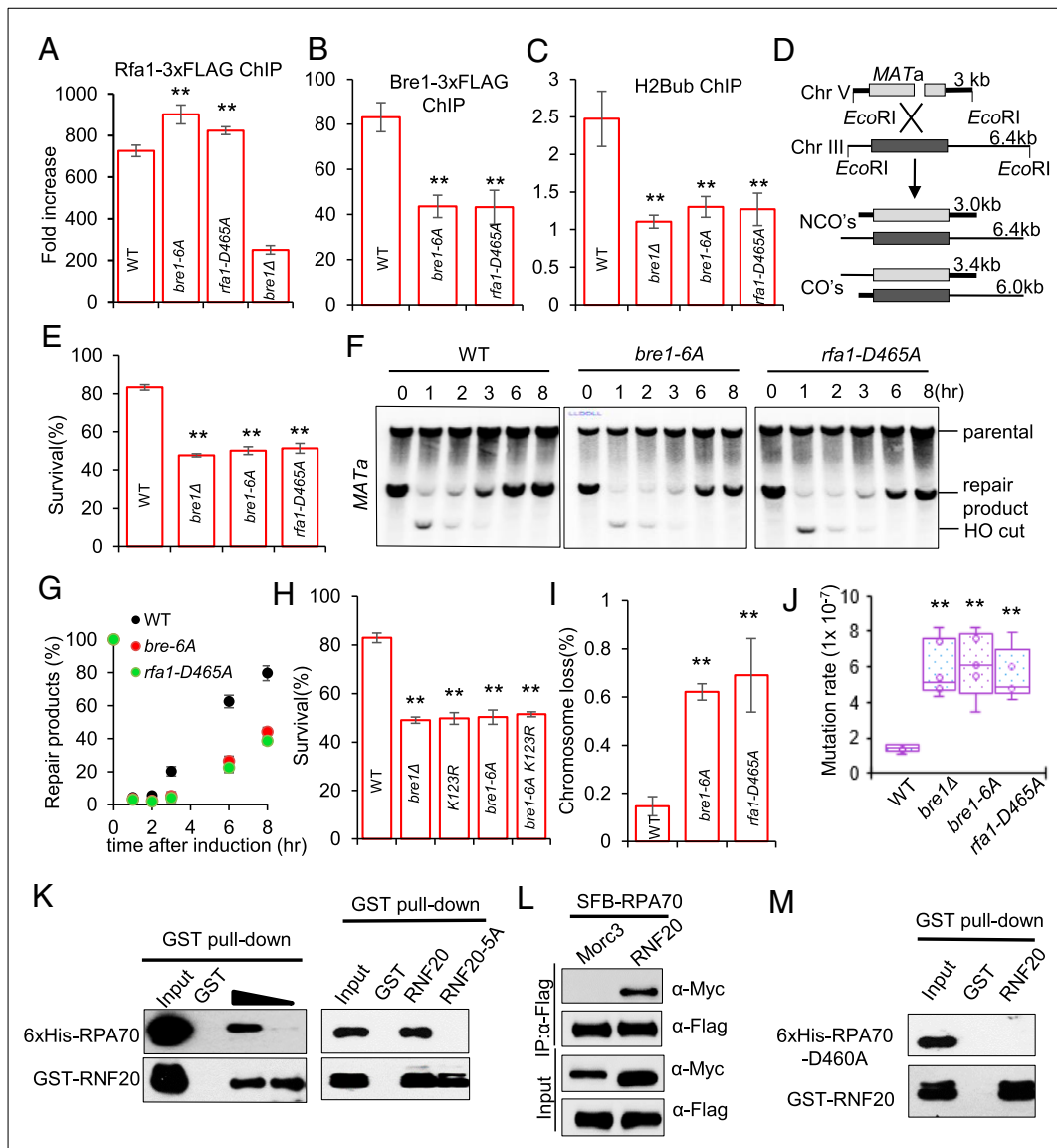


**Fig. 6.** RPA targets Bre1 to DSBs to promote local H2B ubiquitination and repair by HR. (A–C) ChIP qPCR showing the enrichment of RPA-3xFLAG, Bre1-3xFLAG, or H2Bub at 1 kb upstream of the DSB at 4 h after break induction in indicated cells. ChIP signals were normalized to the corresponding input signals, and the derived ChIP/input values were normalized to that of the “0” time-point sample. (D) Scheme showing an ectopic recombination system. CO: cross-over; NCO: noncross-over. (E and H) The survival rate for indicated cells repaired by ectopic recombination. (F and G) Southern blot analysis and quantification of the repair kinetics for indicated cells. (I and J) Plots showing the frequency of chromosome loss and spontaneous mutation, respectively, for indicated yeast strains. Error bars represent SD from at least three independent experiments. \*\* $P < 0.01$  ( $t$  test). (K) GST pull-down assays showing the interaction between human 6xHis-RPA70 and GST-RNF20 or GST-RNF20-5A. The WT or mutant GST-RNF20 (Bottom) was used to capture the associated 6xHis-RPA70 (Top). Anti-His and anti-GST antibodies were used to detect 6xHis-RPA70 and GST-RNF20, respectively. (L) Immunoprecipitation showing the interaction between SFB-tagged RPA70 and Myc-tagged RNF20. The protein Morc3 that does not interact with RPA70 was used as a control. Anti-FLAG antibody was used for the immunoprecipitation. The levels of RPA70 and RNF20 were examined by Western blot using anti-FLAG and anti-Myc antibodies, respectively. (M) GST pull-down assay showing the association between GST-RNF20 and 6xHis-RPA70-D460A. GST-RNF20 (Bottom) was immobilized to beads to capture 6xHis-RPA70-D460A (Top).

association between Bre1 and RPA is important for Rad51 loading and DSB repair by HR. Consistently, the *bre1-6A* mutant cells are hypersensitive to multiple DNA-damaging agents (Fig. 5D). Furthermore, we noted that the survival rate of *bre1-6A* cells is comparable to that seen in *K123R* single mutant or *bre1-6A K123R* double mutant (Fig. 6H), suggesting that the role of RPA–Bre1 interaction in HR repair is executed through affecting H2B ubiquitination.

We also examined the role of this interaction on genome stability by measuring chromosome loss using a system that carries an

extra ~320-kb yeast artificial chromosome (YAC) (47). The loss of YAC was monitored by following the *URA3* and *HIS3* markers on the YAC (47). Approximately 0.2% of WT cells lost the YAC, while this ratio increased over threefold in the *bre1-6A* or *rfa1-D465A* mutant (Fig. 6I). Furthermore, we used the *CAN1* reporter gene to measure the spontaneous mutation frequency in these cells (48). It was reported that *BRE1* deletion does not affect the level of spontaneous mutation (13). However, we noted that mutation frequency is increased by threefold in both *bre1Δ* and *bre1-6A* or *rfa1-D465A* mutant cells relative to that in WT cells

(Fig. 6J). This discrepancy is possibly attributable to the difference in strain background. Together, these results demonstrate that RPA-mediated Bre1–H2Bub exerts versatile roles in guarding genome stability.

**RPA-D465A Mutant Protein Binds ssDNA or Recombination Proteins Normally In Vitro.** To test whether the D465A mutation affects RPA functions, we purified the WT or D465A-mutated RPA complex in which only the N terminus of Rfa1 is fused with a GST tag. By GST pull-down assay, we detected a similar level of Rfa2 or Rfa3 between the WT and mutant RPA complex (SI Appendix, Fig. S12A), suggesting that the mutation does not affect RPA complex formation. Second, using biotin-labeled ssDNA (30 nt) pull-down assay or electrophoretic mobility shift assay, we found that the WT and mutant RPA complex exhibited a similar binding ability for ssDNA (SI Appendix, Fig. S12 B and C). Third, we observed that both the WT and mutant RPA interact with the recombination protein Rad51 or Rad52 at a comparable affinity (SI Appendix, Fig. S12D). Thus, the D465A mutation in RPA does not seem to affect its ability in complex formation, ssDNA binding, or interaction with recombination proteins.

Finally, we compared the global gene expression profiles for the WT, *rfa1-D465A*, and *bre1-6A* cells by RNA sequencing (RNA-Seq). We found that the expression pattern for genes involved in DNA replication, repair, or damage response remains largely unaltered in both mutants as compared to the WT cells (Dataset S1), suggesting that the observed defects in replication, repair, or genome instability in *rfa1-D465A* or *bre1-6A* cells were not resulted from an indirect effect on gene expression.

**Human RNF20 Interacts with RPA in a Conserved Mode.** Given the highly conserved roles of H2Bub across species, we wondered whether RNF20, the human homolog of Bre1, interacts with RPA or not. We expressed human GST-RNF20 and 6xHis-RPA70 recombinant proteins and tested their association by pull-down assay. Notably, we detected a direct interaction between the two proteins (Fig. 6K). Consistently, RPA70 interacts with RNF20 in human cells (HEK293T), as revealed by the immunoprecipitation assay (Fig. 6L). As the residues in Bre1 or RPA that mediate their interaction are conserved across species (SI Appendix, Fig. S4), we assessed whether mutation of the equivalent residues in human RNF20 or RPA70 affects their interaction or not. Importantly, we noted that mutation of the five key residues in RNF20 (L805, E807, E809, L811 and L812, RNF20-5A) or a single residue (D460) in RPA to alanine is sufficient to abolish the association in vitro (Fig. 6 K and M and SI Appendix, Fig. S13 A and B). Thus, we identified a pair of conserved motifs (LxD/ExD/ExLL in Bre1/RNF20 and D465/D460 in yeast or human RPA) that mediate the Bre1/RNF20-RPA interaction. These results raise the possibility that RPA may also recruit RNF20 to replication forks or DSBs in human.

## Discussion

**RPA Couples the Bre1–H2Bub Pathway to DNA Replication and Repair.** Given the critical importance of the Bre1/RNF20-H2Bub pathway in suppressing genome instability and cancer, it is important to elucidate the molecular details for regulating this conserved pathway (15–18, 24, 49). However, it was unclear how this pathway responds to DNA replication and repair. Here, we identify that the ssDNA binding factor RPA acts as the key mediator protein coupling H2B ubiquitination to DNA replication and repair. Bre1 physically interacts with RPA or RPA–ssDNA, and this interaction is critical for Bre1 recruitment and local H2Bub enrichment at replication forks or DSBs (Fig. 7). As a result, disruption of the RPA–Bre1 interaction leads to impaired DNA replication, response to replication stress, and repair by HR, accompanied by increased genome instability and DNA damage sensitivity. Thus, RPA-mediated Bre1 recruitment plays a critical role in preserving

genome stability via coupling the H2Bub pathway to DNA replication and repair.

Recent studies from fission yeast showed that the ubiquitin E2 conjugase Rhp6 (the homolog of yeast Rad6) associates with RPA–ssDNA in vivo and that enrichment of H2Bub at DSBs requires the generation of ssDNA (19). This finding opens the possibility that RPA may also be involved in recruiting the enzymes for H2Bub to DSBs in fission yeast. Although Bre1 can bind the acidic patch of the nucleosome core particle in vitro (43, 44), we observed the specific RPA-dependent targeting of Bre1 to replication forks or DSBs, suggesting that the distribution of Bre1–H2Bub on chromatin is spatiotemporally regulated. Indeed, the association between RPA and Bre1 is affected by the cell cycle and DNA damage (Fig. 1 C and D). It will be interesting to test whether the cell cycle-driving kinase Cdk1 or checkpoint kinases control the association or not. Since the Bre1–H2Bub pathway is also involved in transcription, chromosome segregation, and telomere maintenance, it remains to be determined whether the recruitment of Bre1 to chromatin during these processes depends on RPA or not.

**RPA Acts as a Platform for Recruiting Ubiquitin E3 Ligases.** At stalled forks or DNA damage sites RPA functions as a key sensor of ssDNA to coordinate DNA damage signaling, repair, and recombination (37–39, 50). In addition to protecting ssDNA from nucleases and removing DNA secondary structures, RPA also functions as a key platform for recruiting proteins involved in various DNA transactions. In human cells, RPA interacts with the ubiquitin E3 ligase RFWD3 and targets the enzyme to replication forks, DSBs, or the sites of interstrand cross-links (51–54). In turn, RPA is ubiquitinated by RFWD3 and subsequently degraded to facilitate the removal of RPA from chromatin and the repair of DSBs (53). RFWD3 could act similarly during the fork restart or repair of interstrand cross-links. In yeast, RPA is required for DNA-damage-induced ubiquitination of PCNA, and this is likely achieved through RPA-dependent recruitment of Rad18 to chromatin (55). Here, we identified Bre1 as an E3 ligase recruited by RPA. These results suggest that RPA acts as a hub for integrating the protein ubiquitination system with DNA replication and repair networks across species. It remains to be determined whether Bre1 can in turn act to ubiquitinate RPA and regulates RPA turnover at replication forks or DNA breaks.

Interestingly, the RPA residue (D465 in yeast or D460 in human) that mediates the RPA–Bre1/RNF20 interaction is located in the motif OB-C that forms the trimeric core of RPA (56). However, the site does not appear to interact with RPA2 or

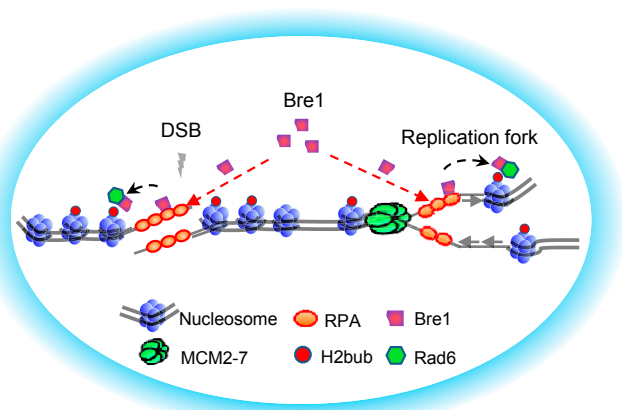


**Fig. 7.** A working model showing RPA-mediated Bre1 recruitment at replication forks or DSBs. RPA recruits Bre1 to DSB ends or replication forks through direct physical interaction. The enrichment of Bre1 at DSBs or replication forks stimulates local H2Bub, thereby ensuring proper DNA replication, response to the replication stress, and repair by HR.

RPA3 and is pointing away from the DNA-binding channel of the OB fold (*SI Appendix, Fig. S14*). Thus, it is available for interacting with other proteins (56). The winged-helix domain of Rfa2 and the basic cleft within the N-terminal OB fold of Rfa1 are known to mediate protein interactions. The latter appears to interact with human ATRIP or RAD9 or yeast Ddc2 in a charge-mediated manner (57, 58). However, the interaction between RPA and Bre1 or RNF20 is obviously different since the involved residues from both proteins are acidic.

**The Recruitment of RNF20/RNF40 in Humans.** In human cells, RNF20 exerts tumor suppression activities. Loss of RNF20/RNF40 and H2Bub was found in several cancers and was linked to an aggressive phenotype (16, 49). The depletion of RNF20 impairs H2Bub, DNA end resection, the recruitment of BRCA1 and RAD51, and the repair by HR (17, 18). How the RNF20/RNF40 complex is targeted to DNA breaks remains to be determined. Although RNF20 interacts with NBS1, the depletion of NBS1 does not affect RNF20 recruitment at DSBs (17). Similarly, PAF1, which is required for RNF20 recruitment in transcription, is dispensable for the DNA-damage-induced RNF20 recruitment and HR repair (59). In light of the conservation of the RPA-Bre1/RNF20 interaction, it will be interesting to test whether RPA recruits RNF20/RNF40 to replication forks or DSBs in human. Our studies provide insights into the mechanism on how the H2Bub pathway responds to DNA replication and repair in eukaryotes and reveal functions of RPA in the spatial-temporal control of H2Bub chromatin landscape and in guarding genome stability.

## Materials and Methods

**Yeast Strains.** All yeast strains used in this study are listed in *SI Appendix, Table S1*. Yeast mutant strains were generated with standard genetic manipulation.

**Mass Spectrometry.** Yeast cells treated with 0.1% MMS (for 1.5 h) were collected and lysed on a bead beater in lysis buffer (100 mM Hepes, pH 8.0, 20 mM MgCl<sub>2</sub>, 150 mM NaCl, 10% glycerol, 0.4% Nonidet P-40, and 0.1 mM ethylenediaminetetraacetic acid [EDTA] plus protease and phosphatase inhibitors). Immunoprecipitated proteins were eluted with a solution containing 3xFLAG peptide. Mass spectrometry analysis was performed as described by Link et al. (60).

**Immunoprecipitation.** Yeast cells culture (A600 ~1.0) with or without MMS treatment were collected and lysed on a bead beater in lysis buffer (100 mM Hepes, pH 8.0, 20 mM MgCl<sub>2</sub>, 150 mM NaCl, 10% glycerol, 0.4% Nonidet P-40, and 0.1 mM EDTA plus protease and phosphatase inhibitors). The supernatant was precleared with protein G-agarose beads, followed by incubation with anti-hemagglutinin (HA) or anti-FLAG antibody at 4 °C overnight with agitation. Protein G-agarose beads were added, and the mixtures were incubated for another 3 h at 4 °C. Subsequently, the beads were washed extensively with lysis buffer at 4 °C. Immunoprecipitated proteins were eluted by boiling beads in 2x sodium dodecyl sulfate (SDS) loading buffer for 5 min.

For RPA70-RNF20 immunoprecipitation, HEK293T cells were cotransfected with SFB-tagged and Myc-tagged constructs. Cells were then lysed with NETN buffer (20 mM Tris-HCl, pH 8.0, 100 mM NaCl, 1 mM EDTA, and 0.5% Nonidet P-40) containing protease inhibitors (1 μg/mL of aprotinin and leupeptin) on ice for 15 min. The cell lysates were centrifuged at 12,000 × g at 4 °C for 5 min, and the resulting supernatants were incubated with Protein A-Sepharose coupled with 1 μg Flag antibody for 2 h at 4 °C with gentle rocking. The bead-bound proteins were washed three times with NETN buffer and resolved on SDS polyacrylamide gel electrophoresis (PAGE).

**Expression of Recombination Proteins and GST Pull-Down Assay.** Expression of the recombination proteins was induced by the addition of 1 mM isopropyl β-D-1-thiogalactopyranoside in *Escherichia coli* BL21 (DE3) at 0.8 optical density at 600 nm. Cells were cultured overnight at 16 °C before harvest. Cells were lysed in lysis buffer (20 mM Tris-HCl, pH 7.4, 50 mM NaCl, 0.5 mM EDTA, and 10% glycerol) by sonication. The lysate was clarified by centrifugation at 12,000 rpm for 30 min at 4 °C. For GST pull-down assay, the recombinant GST-Bre1 immobilized on glutathione agarose beads was then incubated with His-tagged WT or mutant Rfa1 proteins at 4 °C for 4 h on a rotator. The beads were washed extensively with wash buffer (20 mM Tris-HCl, pH 7.4, 200 mM NaCl, 0.5 mM EDTA, and 10% glycerol), and bound proteins were detected by Western blot or Coomassie brilliant blue staining of SDS-PAGE gels.

**Western Blotting.** Western blot was carried out as previously described (61) with the anti-HA (MBL), anti-FLAG (Sigma), or anti-H2B (Abdclone) antibody. Anti-mouse and -rabbit immunoglobulin G horseradish peroxidase-conjugated secondary antibodies were purchased from Santa Cruz Biotechnology. Blots were developed using the Western Blotting substrate (Bio-Rad).

**Streptavidin Pull-Down Assay.** Binding of 6xHis-Bre1 or 6xHis-bre1-6A to RPA-ssDNA was examined using a streptavidin pull-down assay. The 5'-biotinylated oligonucleotides (90 nt) (5'-CGACAGGTATGGCCGTACATGAT-ATCTCGAGCGGTCTGTGCAACTACTCTGAATAGCCGAATCTTAGGGTTAG-GGTTAACA-3') were immobilized on streptavidin MagBeads (GenScript) in TES buffer (10 mM Tris, 1 mM EDTA, and 2 M NaCl, pH 7.5) for 30 min at room temperature. After an extensive wash with 1x phosphate-buffered saline supplemented with 1 mM EDTA, the biotin-ssDNA-streptavidin beads were incubated with 50 nM of purified RPA complex for 30 min at 4 °C. After a wash with the binding buffer (25 mM Hepes, pH 7.5, 15 mM KCl, 150 mM NaCl, 1 mM EDTA, 0.05% Triton X-100, 0.5 dithiothreitol [DTT], and 100 mg/mL bovine serum albumin), purified 6xHis-Bre1 or 6xHis-bre1-6A was added to each sample and incubated for 1 h at 4 °C. Subsequently, the beads were washed with binding buffer, and the bound protein was eluted and detected by Western blot or Coomassie brilliant blue staining.

**ChIP and BrdU ChIP.** Exponentially growing cells (1.2 × 10<sup>7</sup> cells per mL) in YEP-Raffinose medium were subject to DSB induction by adding of 2% galactose. ChIP assays were carried out as previously described with an anti-FLAG or anti-H2Bub antibody (Cell Signaling Technology) (61). BrdU ChIP was carried out as previously described (62).

**Flow Cytometry.** Cells were synchronized in G1 phase followed by released into fresh YPD with or without 200 mM HU. Samples were fixed in 75% precooled ethanol for 2 h at 4 °C. Cells were washed with 50 mM Tris-HCl (pH 8.0) and then resuspended in 300 μL of 50 mM Tris-HCl (pH 8.0) containing 2 mg/mL RNaseA. After incubation at 37 °C for 1 h, cells were harvested and resuspended in 300 μL of 50 mM Tris-HCl (pH 8.0) containing 1 mg/mL proteinase K. Samples were incubated at 55 °C for 1 h before collection. After centrifugation, cells were resuspended in FACS buffer (200 mM Tris-HCl, pH 7.5, 20 mM MgCl<sub>2</sub>, 150 mM NaCl, and 0.02% NaN<sub>3</sub>). One hundred microliters of the cell suspension was mixed with 900 μL of 50 mM Tris-HCl containing 50 μg/mL propidium iodide. Before analysis, samples were sonicated briefly and analyzed with CyAn ADP machinery (Beckman). The data were processed with FlowJo version 10.0.

**Fluorescence Microscopy.** Live cells with or without HU treatment were examined using an Olympus BX53 fluorescence microscope with a 100x oil immersion objective lens and a YFP filter. Fluorescent images were captured using an Olympus DP80 digital camera and processed using Olympus CellSens software. Approximately 300 cells were counted for each sample.

**NCP Ubiquitination Assay.** His-UBA1, his-Rad6, his-Bre1, his-Bre1-6A, GST-Ub, and RPA recombination proteins were expressed in *E. coli* BL21 (DE3). NCP was purified from *bre1Δ* FLAG-H2B cells. For in vitro ubiquitination reactions, 200 nM E1, 72 μM ubiquitin, 6 μM Rad6, 36 μM Bre1, 4 mM ATP, 0.1 mM DTT, and 5 μM NCP were mixed in a reaction buffer volume of 80 μL (50 mM Tris-HCl, pH 8.0, 50 mM NaCl, 50 mM KCl, and 10 mM MgCl<sub>2</sub>) and incubated for 90 min at 30 °C. Reactions were stopped by adding 5x SDS loading buffer and analyzed by 15% SDS-PAGE followed by Western blot with anti-FLAG (F3165; Sigma).

**PFGE.** Yeast growing cells (1.2 × 10<sup>7</sup> cells per mL) were treated with 200 mM HU for 2 h and then released into fresh YPD media. Cells were harvested at the indicated time points. PFGE was performed as previously described with the CHEF-DR III system (Bio-Rad; parameter settings: initial switch time: 20 s, final switch time: 150 s, run time: 26 to 28 h, volts per centimeter: 6 V/cm) (63).

**Spotting Assay and Analysis of Ectopic Recombination.** Spotting assay and the viability or repair kinetics of the HO-induced DSB repair by ectopic recombination were performed as described previously (42, 61).

**Mutation Rate.** The rate of accumulation of CanR mutations was determined as previously described (48).

**RNA-Seq.** RNA-Seq was commercially performed at Meiji Biotech (Shanghai). Three biological repeats were performed for each sample. The RNA-Seq data were deposited into Sequence Read Archive database with accession number PRJNA685864.

**Cell Culture and Transfection.** HEK293T cells were cultured in Dulbecco's modified essential medium containing 10% fetal bovine serum and 1% penicillin and streptomycin and maintained at 37 °C in 5% CO<sub>2</sub>. Cells were transfected with expression vectors using polyethyleneimine according to the manufacturer's instructions.

**Data Availability.** RNA-Seq data have been deposited in the Sequence Read Archive database (accession no. [PRJNA685864](https://doi.org/10.1101/2017.05.01.141111)). All study data are included in the article, [SI Appendix](#), and/or [Dataset S1](#).

1. M. M. Cox *et al.*, The importance of repairing stalled replication forks. *Nature* **404**, 37–41 (2000).
2. H. Técher, S. Koundrioukoff, A. Nicolas, M. Debatisse, The impact of replication stress on replication dynamics and DNA damage in vertebrate cells. *Nat. Rev. Genet.* **18**, 535–550 (2017).
3. J. E. Haber, A life investigating pathways that repair broken chromosomes. *Annu. Rev. Genet.* **50**, 1–28 (2016).
4. S. C. Kowalczykowski, An overview of the molecular mechanisms of recombinational DNA repair. *Cold Spring Harb. Perspect. Biol.* **7**, a016410 (2015).
5. R. Scully, A. Panday, R. Elango, N. A. Willis, DNA double-strand break repair-pathway choice in somatic mammalian cells. *Nat. Rev. Mol. Cell Biol.* **20**, 698–714 (2019).
6. A. Aguilera, T. Garcia-Muse, Causes of genome instability. *Annu. Rev. Genet.* **47**, 1–32 (2013).
7. S. Bhattacharjee, S. Nandi, Choices have consequences: The nexus between DNA repair pathways and genomic instability in cancer. *Clin. Transl. Med.* **5**, 45 (2016).
8. L. S. Symington, R. Rothstein, M. Lisby, Mechanisms and regulation of mitotic recombination in *Saccharomyces cerevisiae*. *Genetics* **198**, 795–835 (2014).
9. L. Zou, S. J. Elledge, Sensing DNA damage through ATRIP recognition of RPA-ssDNA complexes. *Science* **300**, 1542–1548 (2003).
10. M. Lisby, R. Rothstein, Cell biology of mitotic recombination. *Cold Spring Harb. Perspect. Biol.* **7**, a016535 (2015).
11. G. Fuchs, M. Oren, Writing and reading H2B monoubiquitylation. *Biochim. Biophys. Acta* **1839**, 694–701 (2014).
12. S. H. Hung, R. P. Wong, H. D. Ulrich, C. F. Kao, Monoubiquitylation of histone H2B contributes to the bypass of DNA damage during and after DNA replication. *Proc. Natl. Acad. Sci. U.S.A.* **114**, E2205–E2214 (2017).
13. M. R. Northam, K. M. Trujillo, Histone H2B mono-ubiquitylation maintains genomic integrity at stalled replication forks. *Nucleic Acids Res.* **44**, 9245–9255 (2016).
14. K. M. Trujillo, M. A. Osley, A role for H2B ubiquitylation in DNA replication. *Mol. Cell* **48**, 734–746 (2012).
15. S. B. Chernikova, J. A. Dorth, O. V. Razorenova, J. C. Game, J. M. Brown, Deficiency in Bre1 impairs homologous recombination repair and cell cycle checkpoint response to radiation damage in mammalian cells. *Radiat. Res.* **174**, 558–565 (2010).
16. S. B. Chernikova *et al.*, Deficiency in mammalian histone H2B ubiquitin ligase Bre1 (Rnf20/Rnf40) leads to replication stress and chromosomal instability. *Cancer Res.* **72**, 2111–2119 (2012).
17. L. Moyal *et al.*, Requirement of ATM-dependent monoubiquitylation of histone H2B for timely repair of DNA double-strand breaks. *Mol. Cell* **41**, 529–542 (2011).
18. K. Nakamura *et al.*, Regulation of homologous recombination by RNF20-dependent H2B ubiquitination. *Mol. Cell* **41**, 515–528 (2011).
19. M. Zeng *et al.*, CRL4(Wdr70) regulates H2B monoubiquitination and facilitates Exo1-dependent resection. *Nat. Commun.* **7**, 11364 (2016).
20. K. Robzyk, J. Recht, M. A. Osley, Rad6-dependent ubiquitination of histone H2B in yeast. *Science* **287**, 501–504 (2000).
21. A. Wood *et al.*, Bre1, an E3 ubiquitin ligase required for recruitment and substrate selection of Rad6 at a promoter. *Mol. Cell* **11**, 267–274 (2003).
22. B. Zhu *et al.*, Monoubiquitination of human histone H2B: The factors involved and their roles in HOX gene regulation. *Mol. Cell* **20**, 601–611 (2005).
23. B. Fierz *et al.*, Histone H2B ubiquitylation disrupts local and higher-order chromatin compaction. *Nat. Chem. Biol.* **7**, 113–119 (2011).
24. S. Zheng *et al.*, Bre1-dependent H2B ubiquitination promotes homologous recombination by stimulating histone eviction at DNA breaks. *Nucleic Acids Res.* **46**, 11326–11339 (2018).
25. M. K. Ma, C. Heath, A. Hair, A. G. West, Histone crosstalk directed by H2B ubiquitination is required for chromatin boundary integrity. *PLoS Genet.* **7**, e1002175 (2011).
26. L. Sadeghi, L. Siggens, J. P. Svensson, K. Ekwall, Centromeric histone H2B monoubiquitination promotes noncoding transcription and chromatin integrity. *Nat. Struct. Mol. Biol.* **21**, 236–243 (2014).
27. Z. Wu *et al.*, Rad6-Bre1-mediated H2B ubiquitination regulates telomere replication by promoting telomere-end resection. *Nucleic Acids Res.* **45**, 3308–3322 (2017).
28. K. Yamashita, M. Shinohara, A. Shinohara, Rad6-Bre1-mediated histone H2B ubiquitylation modulates the formation of double-strand breaks during meiosis. *Proc. Natl. Acad. Sci. U.S.A.* **101**, 11380–11385 (2004).
29. M. Zofall, S. I. Grewal, HULC, a histone H2B ubiquitinating complex, modulates heterochromatin independent of histone methylation in fission yeast. *J. Biol. Chem.* **282**, 14065–14072 (2007).
30. W. Zhang, C. H. L. Yeung, L. Wu, K. W. Y. Yuen, E3 ubiquitin ligase Bre1 couples sister chromatid cohesion establishment to DNA replication in *Saccharomyces cerevisiae*. *eLife* **6**, e28231 (2017).
31. W. W. Hwang *et al.*, A conserved RING finger protein required for histone H2B monoubiquitination and cell size control. *Mol. Cell* **11**, 261–266 (2003).
32. Z. W. Sun, C. D. Allis, Ubiquitination of histone H2B regulates H3 methylation and gene silencing in yeast. *Nature* **418**, 104–108 (2002).

**ACKNOWLEDGMENTS.** We thank Dr. Douglas Koshland (University of California, Berkeley) and Dr. Qing Li (Peking University) for providing yeast strains, Dr. Xiangwei He (Zhejiang University) for critical reading of the manuscript, and Dr. He He (Wuhan University) for assistance with mass spectrometry analysis. This work is supported by National Natural Science Foundation of China grants 31872808, 32070573, and 31671294; National Basic Key Research Program of China grant 2015CB910602; and the Genetics Course Program funded by Wuhan University Graduate School (X.C.).

33. C. C. So, S. Ramachandran, A. Martin, E3 ubiquitin ligases RNF20 and RNF40 are required for double-stranded break (DSB) repair: Evidence for monoubiquitination of histone H2B lysine 120 as a novel Axis of DSB signaling and repair. *Mol. Cell. Biol.* **39**, e00488-18 (2019).
34. J. C. Game, S. B. Chernikova, The role of RAD6 in recombinational repair, checkpoints and meiosis via histone modification. *DNA Repair (Amst.)* **8**, 470–482 (2009).
35. J. C. Game, M. S. Williamson, T. Spicakova, J. M. Brown, The RAD6/BRE1 histone modification pathway in *Saccharomyces* confers radiation resistance through a RAD51-dependent process that is independent of RAD18. *Genetics* **173**, 1951–1968 (2006).
36. D. Faucher, R. J. Wellinger, Methylated H3K4, a transcription-associated histone modification, is involved in the DNA damage response pathway. *PLoS Genet.* **6**, e1001082 (2010).
37. R. Chen, M. S. Wold, Replication protein A: Single-stranded DNA's first responder: Dynamic DNA-interactions allow replication protein A to direct single-strand DNA intermediates into different pathways for synthesis or repair. *BioEssays* **36**, 1156–1161 (2014).
38. A. Maréchal, L. Zou, RPA-coated single-stranded DNA as a platform for post-translational modifications in the DNA damage response. *Cell Res.* **25**, 9–23 (2015).
39. M. S. Wold, Replication protein A: A heterotrimeric, single-stranded DNA-binding protein required for eukaryotic DNA metabolism. *Annu. Rev. Biochem.* **66**, 61–92 (1997).
40. B. Pardo, L. Crabbé, P. Pasero, Signaling pathways of replication stress in yeast. *FEMS Yeast Res.* **17** (2017).
41. S. E. Lee *et al.*, *Saccharomyces* Ku70, mre11/rad50 and RPA proteins regulate adaptation to G2/M arrest after DNA damage. *Cell* **94**, 399–409 (1998).
42. Z. Zhu, W. H. Chung, E. Y. Shim, S. E. Lee, G. Ira, Sgs1 helicase and two nucleases Dna2 and Exo1 resect DNA double-strand break ends. *Cell* **134**, 981–994 (2008).
43. L. D. Gallego *et al.*, Structural mechanism for the recognition and ubiquitination of a single nucleosome residue by Rad6-Bre1. *Proc. Natl. Acad. Sci. U.S.A.* **113**, 10553–10558 (2016).
44. E. Turco, L. D. Gallego, M. Schneider, A. Köhler, Monoubiquitination of histone H2B is intrinsic to the Bre1 RING domain-Rad6 interaction and augmented by a second Rad6-binding site on Bre1. *J. Biol. Chem.* **290**, 5298–5310 (2015).
45. M. Giannattasio, F. Lazzaro, P. Plevani, M. Muzi-Falconi, The DNA damage checkpoint response requires histone H2B ubiquitination by Rad6-Bre1 and H3 methylation by Dot1. *J. Biol. Chem.* **280**, 9879–9886 (2005).
46. G. Ira, A. Malkova, G. Liberi, M. Foiani, J. E. Haber, Srs2 and Sgs1-Top3 suppress crossovers during double-strand break repair in yeast. *Cell* **115**, 401–411 (2003).
47. L. Wahba, J. D. Amon, D. Koshland, M. Vuica-Ross, RNase H and multiple RNA biogenesis factors cooperate to prevent RNA:DNA hybrids from generating genome instability. *Mol. Cell* **44**, 978–988 (2011).
48. M. E. Huang, A. G. Rio, A. Nicolas, R. D. Kolodner, A genomewide screen in *Saccharomyces cerevisiae* for genes that suppress the accumulation of mutations. *Proc. Natl. Acad. Sci. U.S.A.* **100**, 11529–11534 (2003).
49. G. Sethi, M. K. Shanmugam, F. Arfuso, A. P. Kumar, Role of RNF20 in cancer development and progression—A comprehensive review. *Biosci. Rep.* **38**, BSR20171287 (2018).
50. L. I. Toledo *et al.*, ATR prohibits replication catastrophe by preventing global exhaustion of RPA. *Cell* **155**, 1088–1103 (2013).
51. A. E. Elia *et al.*, RFWFD3-dependent ubiquitination of RPA regulates repair at stalled replication forks. *Mol. Cell* **60**, 280–293 (2015).
52. L. Feeney *et al.*, RPA-mediated recruitment of the E3 ligase RFWFD3 is vital for inter-strand crosslink repair and human health. *Mol. Cell* **66**, 610–621.e4 (2017).
53. S. Inano *et al.*, RFWFD3-mediated ubiquitination promotes timely removal of both RPA and RAD51 from DNA damage sites to facilitate homologous recombination. *Mol. Cell* **66**, 622–634.e8 (2017).
54. Y. C. Lin *et al.*, PCNA-mediated stabilization of E3 ligase RFWFD3 at the replication fork is essential for DNA replication. *Proc. Natl. Acad. Sci. U.S.A.* **115**, 13282–13287 (2018).
55. A. A. Davies, D. Huttner, Y. Daigaku, S. Chen, H. D. Ulrich, Activation of ubiquitinating-dependent DNA damage bypass is mediated by replication protein a. *Mol. Cell* **29**, 625–636 (2008).
56. E. Bochkareva, S. Korolev, S. P. Lees-Miller, A. Bochkarev, Structure of the RPA trimerization core and its role in the multistep DNA-binding mechanism of RPA. *EMBO J.* **21**, 1855–1863 (2002).
57. X. Xu *et al.*, The basic cleft of RPA70N binds multiple checkpoint proteins, including RAD9, to regulate ATR signaling. *Mol. Cell. Biol.* **28**, 7345–7353 (2008).
58. H. L. Ball *et al.*, Function of a conserved checkpoint recruitment domain in ATRIP proteins. *Mol. Cell. Biol.* **27**, 3367–3377 (2007).
59. D. V. Oliveira *et al.*, Histone chaperone FACT regulates homologous recombination by chromatin remodeling through interaction with RNF20. *J. Cell Sci.* **127**, 763–772 (2014).
60. A. J. Link *et al.*, Direct analysis of protein complexes using mass spectrometry. *Nat. Biotechnol.* **17**, 676–682 (1999).
61. X. Chen *et al.*, The Fun30 nucleosome remodeller promotes resection of DNA double-strand break ends. *Nature* **489**, 576–580 (2012).
62. C. Yu *et al.*, Strand-specific analysis shows protein binding at replication forks and PCNA unloading from lagging strands when forks stall. *Mol. Cell* **56**, 551–563 (2014).
63. L. Maringe, D. Lydall, Pulsed-field gel electrophoresis of budding yeast chromosomes. *Methods Mol. Biol.* **313**, 65–73 (2006).